

## Multiple-scattering effects in polarization-dependent surface XAFS

N. Binsted and D. Norman

*Science and Engineering Research Council, Daresbury Laboratory, Warrington WA4 4AD, United Kingdom*

(Received 1 February 1994)

The effect of multiple scattering (MS) on the x-ray absorption fine structure (XAFS) spectrum is investigated by means of calculations using the full curved wave theory with exact polarization dependence and including all orders of MS up to five. We performed model calculations for the hypothetical half-monolayer  $c(2 \times 2)$  overlayer of atomic O on an unreconstructed Cu(100) or (110) surface and assuming adsorption in hollow, bridge or atop sites at an O-Cu distance of 1.85 Å. From these calculations it is found that MS is important for some adsorption geometries and polarization directions. Failure to include at least the dominant double scattering terms in an analysis may result in errors in the parameters for some distances beyond the nearest neighbors. We derive general rules for when MS is likely to influence surface EXAFS (extended x-ray absorption fine structure) spectra. Most of the significant three-atom paths involve either one small ( $< 45^\circ$ ) or large ( $> 150^\circ$ ) scattering angle, with the most favorable geometry for MS being when forward scattering occurs at a light atom and backscattering at a heavy atom. The dominant MS paths involve the shortest bonds in the material. Contributions tend to be largest where the  $\epsilon$  vector is roughly parallel to one of these bonds, and there is often a substantial polarization dependence to the MS terms. Multiple-scattering effects are likely to be strongest when adsorbate atoms occupy sites close to coplanar with the surface. The presence of MS peaks at high- $R$  in an experimental spectrum is a useful indication of high symmetry and relatively long-range order in surface structures. We also show that much of the near-edge region can be fitted using an EXAFS algorithm which includes a sufficiently small number of multiple-scattering paths to make routine calculation feasible, provided that the exact curved wave polarization dependence is included.

### I. INTRODUCTION

Surface extended x-ray-absorption fine structure (EXAFS) is well established as one of the battery of techniques for studying adsorbate-substrate geometries.<sup>1-3</sup> The interference between outgoing and backscattered photoelectron waves gives oscillations in the x-ray-absorption coefficient whose frequency is inversely related to the adsorbate-substrate distance, and whose amplitude carries information on the coordination number. On single-crystal surfaces, measurement of the polarization-dependent amplitude usually yields the adsorption site. Although experimentally difficult, needing an intense synchrotron-radiation x-ray source, surface EXAFS has the appealing advantage that a straightforward analysis appears to be possible using Fourier transformation of the experimental data. Such analysis, however, assumes that the photoelectron undergoes only single scattering (SS), with no paths involving two or more neighboring atoms. This assumption is not always valid, and the circumstances in which the SS approximation breaks down have been quite extensively explored for bulk systems. As the quality of surface EXAFS data has improved over the years, tempting investigators to interpret more distant neighbor shells, it has become increasingly important to understand multiple-scattering (MS) effects in surface systems. The intention of this paper is to investigate some typical adsorption geometries and derive the general rules for when MS has to be taken into account for surface studies.

The importance of multiple scattering of the photoelec-

tron in EXAFS has been recognized ever since the quantitative theory was established in the classic paper by Lee and Pendry.<sup>4</sup> In the x-ray-absorption near-edge structure [(XANES), otherwise known as near-edge x-ray-absorption fine structure] where the low-energy photoelectron is strongly scattered, MS is important in almost all materials,<sup>5</sup> including surface adsorbate systems.<sup>6,7</sup> At higher energies, in the EXAFS region, the photoelectron is less strongly scattered and single scattering dominates in most cases. However there are certain geometries of scattering atoms where multiple scattering may be significant even at electron kinetic energies as high as 1 keV or more. The first is where two or more scattering atoms are collinear, when strong forward scattering "focuses" the outgoing photoelectron onto the second atom, as is seen, for instance, in the fourth shell of face-centered-cubic metals.<sup>4</sup> Similar effects might also be found in surface EXAFS if an adsorbate occupied a lattice site, as with epitaxial layers, but such contributions are less likely for other sites or with reconstructed surfaces because of the reduced symmetry. The second geometry in which multiple scattering at high energies is most pronounced, is where large bond angles are accompanied by very short interatomic bonds. Such bonds, as found for instance with C-O in transition-metal carbonyls ( $\sim 1.05$  Å), markedly enhance the magnitude of MS relative to SS for contributions of similar path length.<sup>8,9</sup>

A third situation where high-energy multiple scattering is important was recognized for surfaces by Arvanitis, Baberschke, and Wenzel<sup>10</sup> who showed the effect of double scattering paths (second-order scattering) involving

an adsorbate in a bridge site and the two underlying substrate atoms in the systems  $(2 \times 1)\text{O}/\text{Ni}(110)$  and  $(2 \times 1)\text{O}/\text{Cu}(110)$ . The geometry differs from the previous case in having two backscattering events for double scattering paths and is associated with large (close to backscattering) rather than small (close to forward scattering) angles. Arvanitis, Baberschke, and Wenzel<sup>10</sup> used a scheme due to Boland, Crane, and Baldeschweiler<sup>11</sup> which calculates amplitudes of significant MS contributions within the plane-wave approximation. They showed that multiple scattering is significant in the EXAFS region and that, with high-quality data, it may be possible to distinguish between different models for a surface reconstruction by analyzing the MS paths.

Thus, three general classes of system have been identified where multiple scattering at high electron energies is significant. It is also important to understand the magnitude of MS at low energies as the edge region is approached. This is particularly useful in surface x-ray-absorption spectroscopy, where the data are frequently noisy and limited in range. The best signal-to-noise ratio is obtained in the low-energy region and it is desirable to use as much as possible of the near-edge region in a structural analysis. Fitting the XANES region depends not only on including sufficient MS paths but also on ensuring that calculated phase shifts are valid throughout the spectrum,<sup>12</sup> and that the background subtraction is adequate. Although not trivial, it is possible to satisfy these two criteria, and so we shall demonstrate both where it is essential to include MS in fitting the high-energy data, and also that much of the XANES region can be fitted using an EXAFS algorithm which includes a sufficiently small number of MS paths to make routine calculation feasible.

In Sec. II we outline the terms in the EXAFS equation and describe the way in which these factors were taken into account in performing the calculations. We explain how curved wave effects and the exact polarization dependence are treated, which MS paths are included in our calculation, how thermal motion is introduced, and our method of calculating scattering phase shifts. Results have been calculated for 13 different combinations of adsorbate site and polarization direction, five of which are contained in Sec. III. Some of this work has been briefly reported elsewhere.<sup>13</sup> In Sec. IV we discuss the results and bring out general guidelines for situations where MS will affect surface EXAFS. Some examples are given of particular surface systems where MS might influence the analysis.

## II. THEORETICAL CALCULATIONS

The EXAFS function  $\chi(E)$  is defined by

$$\chi(E) = \frac{\mu(E)}{\mu_0(E)} - 1,$$

where  $\mu(E)$  is the portion of the x-ray absorption that is due to the edge under consideration, and  $\mu_0(E)$  is the background absorption arising from all the other edges in the system. Within the dipole approximation  $\mu$  can be given by Fermi's Golden rule,

$$\mu \sim \sum |\langle \Psi_f | \epsilon \cdot \mathbf{r} | \Psi_i \rangle|^2 \delta(E_i + h\nu - E_f), \quad (1)$$

where  $\epsilon$  is the polarization vector of the electric field,  $\mathbf{r}$  is a direction vector, and the  $\delta$  function expresses the selection rule relating the energies of the initial and final states ( $E_i$  and  $E_f$ ) and the photon energy  $h\nu$ . For an isolated atom the final state (a core hole plus the emitted photoelectron) can be treated simply as a spherical wave, and the wave function given by a real radial part multiplied by a spherical harmonic. In a condensed sample the outgoing photoelectron is scattered by neighboring atoms, giving rise to EXAFS. In this case the final-state wave function becomes<sup>8,14</sup>

$$|\Psi_f\rangle = \sum_{LM} \begin{pmatrix} I + Z_{L' M'} \\ L M \end{pmatrix} |LM\rangle,$$

where  $I$  is a unit matrix and  $Z$  is the scattering matrix. Here we consider only  $K$  edges, where, because there is only one allowed final state (with angular momentum  $l_f=1$ ), the exact expression for the EXAFS  $\chi$  is given by<sup>8,14</sup>

$$\chi = A \frac{2}{(2l_f + 1)} \text{Re} M Z M^* \exp(2i\delta_{l_f}), \quad (2)$$

where  $\text{Re}$  indicates the real part of the expression and  $\delta_{l_f}$  is the  $l_f=1$  phase shift. The first term  $A$  accounts for the reduction of amplitude caused by multielectron events such as shake-up and shake-off. Vibrational effects are included through the temperature-dependent  $T$  matrix,

$$T_l(k) = \frac{1}{2} \{ \exp(2i\delta_l) - 1 \},$$

as in Sec. II D below. The direction vector  $M$  is defined below [Eq. (3)]. The matrix  $Z$ , which contains all the scattering information, is expanded to  $n$  orders of multiple scattering, exactly as defined by Lee and Pendry.<sup>4</sup> Much of this formalism is standard, and in the rest of this section we concentrate on the critical parts of the theory, particularly emphasizing where our treatment differs from those used elsewhere.

### A. Curved wave

Although the plane-wave formalism of EXAFS may be adequate for single scattering at high energies, it is not acceptable for multiple scattering even at electron energies as high as several keV. Spherical wave scattering is mathematically complex, mainly because of the coupling of angular momenta, and several authors have introduced so-called separable approximations<sup>14-20</sup> and other formalisms<sup>21</sup> to make the task tractable. They appear to work through most of the EXAFS range, but most of the representations introduce errors that increase with energy,<sup>22</sup> particularly for short (near-neighbor) distances, and they also break down close to the edge except in some favorable cases.<sup>23,24</sup> We therefore use the full curved (spherical) wave theory throughout, although computational limitations have forced us to restrict the number of angular momentum terms used (see Sec. II E below).

### B. Polarization dependence of coordination number

For our applications to the surfaces of single crystals, it is important to note that the exact polarization dependence is used. This enters the mathematics in Eq. (1) via the expansion of the dot product  $\epsilon \cdot r$  in terms of spherical harmonics,<sup>14</sup> with a direction vector  $M$  given in terms of beam direction  $(\vartheta, \varphi)$  and polarization  $(\omega)$  angles, using Gurman's<sup>14</sup> notation, by

$$M = |A - B - A^*|, \quad (3)$$

where

$$A = \exp(-i\varphi)(i \cos\omega - \sin\omega \cos\vartheta) \quad (4)$$

and

$$B = -\sqrt{2} \sin\omega \cos\vartheta. \quad (5)$$

Elsewhere, polarization dependence is usually treated by use of an apparent occupation number

$$N^* = N \cos^2\alpha, \quad (6)$$

where  $\alpha$  is the angle between the bond and the  $\epsilon$  vector. This is valid in the small atom and plane-wave approximations. In spherical wave theory, however, it is not exact,<sup>25-28</sup> and although Eq. (6) is a good approximation throughout the EXAFS region, it breaks down close to the edge and gives significant errors. We therefore use the exact polarization dependence given above [Eqs. (2)-(5)], as is also done in XANES calculations.<sup>29</sup> For this it is necessary to calculate the off-diagonal terms in  $Z_{mm}$ , which precludes the use of any of the published approximations to MS, such as Refs. 14, 17, and 18.

### C. Scattering paths

The number of MS paths in a solid is effectively infinite, and some limits have to be placed on the number of terms used. EXAFS amplitudes decay inversely with the product of the lengths of each leg in the scattering path, and are further restricted by the final-state lifetime, which results in an effective mean free path for the photoelectron. We therefore introduce a maximum path length, which, for ease of computation, is usually lower for MS than for SS. Exceptionally EXAFS data show evidence for shells up to 15 Å (30 Å path length),<sup>30</sup> but for most surface systems, contributions from shells beyond about 5 Å are small, and we consider a maximum path length of 15 Å for SS and 13 Å for MS to be sufficient.

This restriction on the path length limits the possible number of orders of scattering to five for the systems discussed here. Fifth-order terms can be significant in the edge region,<sup>31</sup> while seventh-order scattering is needed<sup>32</sup> to give reasonable agreement with a band-structure calculation for bulk copper in the medium energy range (20-190 eV). It is clear that care has to be taken to include sufficient terms for such close-packed, high symmetry, systems. Short bond length molecules, where up to 13th-order backscattering may be necessary to describe the strong low-energy shape resonances,<sup>32</sup> obviously represent an extreme situation. However, we believe that

few, if any, surface structures will exhibit EXAFS spectra with higher than fifth-order MS. We are also encouraged by the generally good agreement obtained between our multiple scattering EXAFS and matrix inversion methods,<sup>5,33</sup> where MS to all orders is included.

A more serious restriction is in the number of atoms involved in each scattering path.<sup>34</sup> For these calculations, for each unique pair of atoms we calculate all the second- to fifth-order terms, and in each triplet we include all third- to fifth-order terms. Fourth- and fifth-order terms in four and five atom groups are therefore excluded. These terms may matter in materials such as Cr(CO)<sub>6</sub> (Ref. 31) where the center of symmetry generates groups of five collinear atoms and where bond distances are short. We are not however aware of any comparable situations in surface EXAFS, at least for atomic adsorbates, and we believe sufficient terms have been included to calculate both the near-edge and high-energy regions within the resolution determined by the lifetime of the final state.

### D. Thermal motion

Multiple-scattering amplitudes depend very much on the treatment of disorder in the system. Rather than use the correct form of temperature-dependent  $T$  matrix, we follow most other workers in using the plane-wave approximation to the temperature dependence of the scattering amplitude which relates the EXAFS at temperature  $\tau$  to that at 0 K by

$$T_l^\tau = T_l^0 \exp(-2\sigma^2 k^2),$$

where  $\sigma^2$  is the Debye-Waller-like term for the mean-square difference in neighbor distance. This treatment results in an apparent shortening of distances with increasing disorder.<sup>35-37</sup> There is no unanimity on how to model disorder in MS calculations. The assumptions we have made are (a) that the only thermal motion is in the relative displacement of a scattering atom and the central atom, and (b) that the effect of a displacement  $\sigma$  is proportional to the relative change it induces in the path length.

This yields a new expression

$$\sigma_{MS}^2 = \cos^4(\gamma/2)\sigma_{SS}^2,$$

where  $\gamma$  is the scattering angle, which is  $\pi$  minus the bond angle. For example, in a system of two collinear scattering atoms, the scattering angle  $\gamma$  is zero at the first atom, and the Debye-Waller-like term is 0, while for backscattering at the second atom, the single-scattering value is used. Although crude, we have found in practice that this treatment gives excellent results for the rigid  $\pi$ -bonded complexes where MS is strongest, with accurate simulations of experimental data, and distances close to crystallographic values. For other systems, this treatment is likely to underestimate the effect of disorder. An important point is that no additional variables are introduced, apart from the scattering angles, making a MS analysis a more severe test of a structural model, particularly when constrained or restrained refinement is used to increase the overdeterminacy of the refinement.<sup>38</sup> For-

tunately, although the effect of disorder is very large at high energy (for fifth-order scattering it involves the product of five terms, all  $\ll 1$ ), at low energy where MS is strongest, the effect is less marked. Thus our treatment of disorder is not accurate but will not strongly affect our results. For the purposes of our calculations we have assumed that  $2\sigma^2$  is  $0.008 \text{ \AA}^2$  for the strongly correlated first shell and  $0.016 \text{ \AA}^2$  for the other shells. These values are typical of our own and published simulations for low or medium atomic number elements on transition-metal surfaces.

### E. Partial waves and phase shifts

The calculation of accurate scattering phase shifts is very important when simulating experimental spectra. Previously<sup>31</sup> we have used ground-state potentials calculated according to the Mattheis prescription<sup>39</sup> using relativistic Hartree-Fock atomic charge densities or potentials generated from linearized muffin-tin-orbital band-structure calculations. In this scheme a constant complex self-energy is used to calculate the photoelectron wave vector which includes effects due to the lifetime of the final state. For heavy elements and for most metals, however, we have found—in common with many other workers—that excited-state potentials<sup>40,41</sup> using a Hedin-Lundqvist exchange<sup>42</sup> and an energy-dependent self-energy<sup>15,43,44</sup> give phase shifts resulting in better fits for a number of systems, including a range of transition-metal sulfides where the reliability of calculated phase shifts had been questioned.<sup>45,46</sup> At present, however, we have not been able to obtain realistic results in the edge region using Hedin-Lundqvist potentials, and as we wish to show how scattering contributions contribute to the edge-region we use phase shifts calculated for Mattheis ground-state potentials throughout.

The number of angular momentum terms  $l_{\max}$  included should be<sup>47</sup> at least  $R_{\text{mt}} \times k_{\max}$ , with  $R_{\text{mt}}$  the muffin tin radius and  $k_{\max}$  the maximum value of wave vector  $k$ . This yields a typical value for a first row transition-metal scatterer of  $l_{\max} \sim 25$  at 800 eV. In practice, values of  $l_{\max}$  of 18 for SS and 12 for MS are acceptable, the main error being that vibrational amplitudes  $\sigma^2$  appear to be smaller than they should be. Values of  $l_{\max}$  of, say, 12 and 6 respectively, will result in significant errors in bond lengths. As this paper treats multiple scattering in a very general way, without the benefit of the fast algorithms developed for the most commonly used cases,<sup>8,48</sup> we have had to restrict the number of phase shifts to an  $l_{\max}$  of 5 in all the calculations presented here. Although inadequate in practice except at low energy, this should not affect our conclusions on the relative magnitudes of multiple- and single-scattering effects.

## III. RESULTS

Calculations were performed for a typical light atom adsorbate (O) adsorbed as a hypothetical half-monolayer  $c(2 \times 2)$  overlayer in idealized sites on a typical transition-metal (Cu) (100) or (110) surface. The nearest-neighbor distance was kept at  $1.85 \text{ \AA}$ , the same as the Cu-O distance in  $\text{Cu}_2\text{O}$ , for all adsorption sites. We are

aware that the structure of oxygen on copper single-crystal surfaces is often complex and is still controversial,<sup>49</sup> but our concern here was to draw general conclusions concerning the importance of MS rather than precisely imitate experimental data. We therefore chose to adopt simple models which facilitate comparisons between sites. In each case the energy range was taken to be from 3 to 650 eV above the muffin-tin zero ( $k = 1$  to  $13 \text{ \AA}^{-1}$ ). Neighbor distances up to  $7.5 \text{ \AA}$  were included for SS, with MS to fifth order for path lengths to  $13 \text{ \AA}$ . The lifetime of the final state was accounted for by a constant imaginary potential of  $-3 \text{ eV}$ , about  $1 \text{ eV}$  smaller in magnitude than a typical value for Cu metal,<sup>4</sup> reflecting the smaller width of the O K core hole.<sup>50</sup> Calculations were performed with the x-ray beam at normal incidence, aligned along the two orthogonal azimuths, where applicable, and at grazing incidence.

A comment on the terminology is appropriate here. "Shell" is used to mean a set of atoms generated by operation of the point-symmetry operator. Fourier transformation of the EXAFS  $\chi(k)$  gives a spectrum  $F(R)$ , analogous to a radial distribution function, with peaks at certain distances. These peaks in the Fourier transform, even in single scattering, may not be obviously related to shell radii. At higher  $R$  values, the shape of  $F(R)$  is distorted by factors such as the data range transformed, truncation errors, and inadequacies of phase correction. Two shells may have the same, or similar, radii, and many shells contribute to most peaks. It is therefore important to note that shells and peaks are not synonymous.

We have performed calculations for 13 different geometries (three polarization directions for five adsorption sites, two of  $C_{4v}$  and three of  $C_{2v}$  symmetry), the results of which are shown in Fig. 1 ( $k^2$  weighted EXAFS) and Fig. 2 (Fourier transforms). The full calculation including MS to fifth order is shown as a solid line, with the SS contribution as a dotted line. In the interests of brevity, we describe here only the results for the O/Cu(100) fourfold hollow and O/Cu(110) long bridge sites: these are the sites where MS has the greatest effect. Details of the results for the other geometries are available from the authors. The calculations included all the atoms whose coordinates are listed in Tables I and II.

### A. (100) surface: Fourfold hollow site ( $C_{4v}$ symmetry)

$$\varepsilon \| x \text{ or } \varepsilon \| y \text{ (normal incidence)}$$

The spectrum is dominated by the SS contribution of the four copper atoms at  $1.85 \text{ \AA}$ . Other SS contributions are fairly weak, but give rise to two peaks around  $R = 3.4$  and  $R = 4.0 \text{ \AA}$ . Multiple scattering is strong in comparison to SS from shells beyond the first and results in significant structure throughout the energy range of the spectrum. Indeed, the MS contribution at high  $k$  is greater than for any of the other structures considered in this work.

The  $3.4\text{-\AA}$  SS peak is substantially modified in the full calculation by the  $\{0-1-1-0\}$  (short path) and  $\{0-1-1-0\}$  (long path),  $\{0-1-4-0\}$  and  $\{0-1-4-1-0\}$  contributions, with

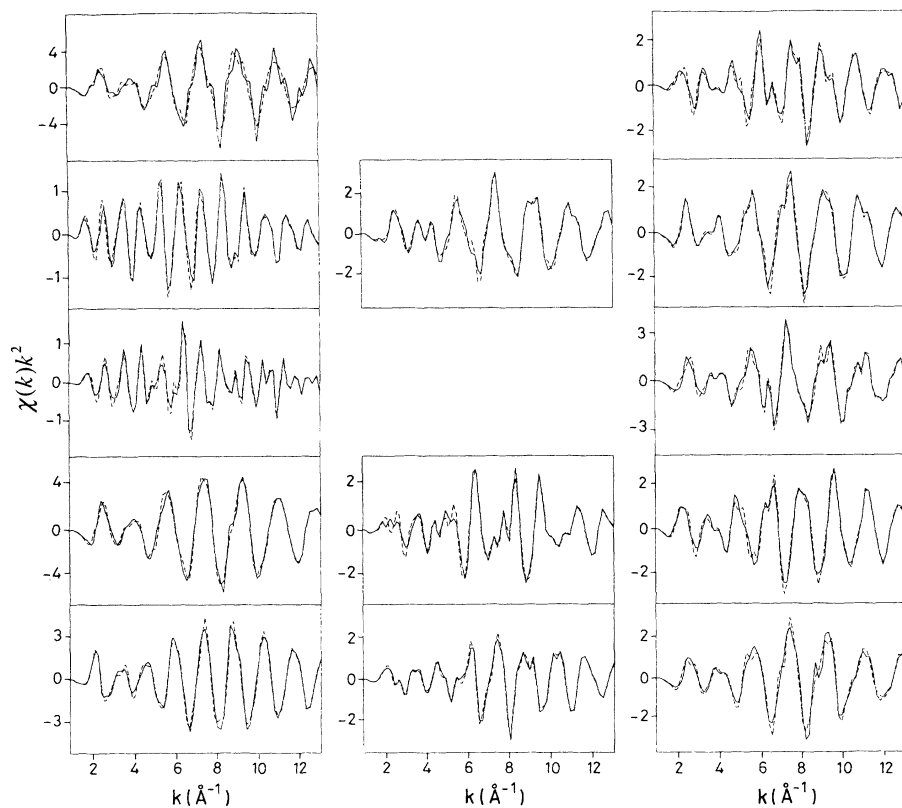


FIG. 1. Calculated EXAFS spectra  $\chi(k)k^2$  for the hypothetical  $c(2 \times 2)$  coverage of O atoms on a Cu single-crystal surface. The three columns, reading from left to right, are with the polarization vector  $\epsilon||x$ ,  $\epsilon||y$ , and  $\epsilon||z$ , respectively. The five rows, reading from top to bottom, are for the O atoms occupying (a) fourfold hollow sites on the (100) face; (b) symmetric bridge sites on the (100) face; (c) atop sites on the (100) face; (d) the  $C_{2v}$  hollow sites on the (110) face; and (e) the long bridge sites on the (110) face. The two missing panels are for the two sites with  $C_{4v}$  symmetry, where  $\epsilon||x$  and  $\epsilon||y$  are symmetrically equivalent. The full lines result from the complete calculation with all orders of multiple scattering up to five, and the dashed lines are with single scattering only.

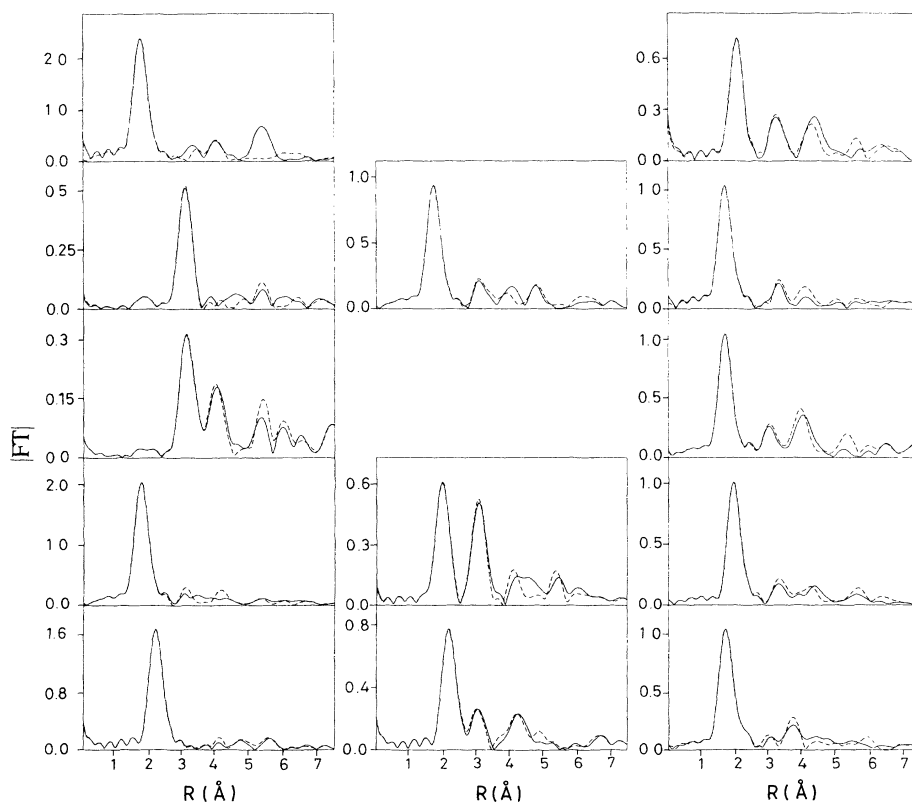


FIG. 2. Fourier transforms of the EXAFS spectra from Fig. 1. The distance scale is corrected for the phase shift from the central atom and a single Cu back-scattering atom.

TABLE I. Atom types and distances for our model geometry of O/Cu(100) fourfold hollow site ( $C_{4v}$  symmetry). All of the atoms listed in the table were included in the full MS calculations. The oxygen central (absorber) atom is at (0,0,0).

Shell	$N$	Atom	$R$ (Å)	$x$ (Å)	$y$ (Å)	$z$ (Å)
1	4	Cu	1.850	1.278	1.278	-0.395
2	1	Cu	2.202	0.000	0.000	-2.202
3	4	Cu	3.374	2.556	0.000	-2.202
4	4	O	3.615	2.556	2.556	0.000
5	8	Cu	4.001	3.834	1.278	-0.395
6	4	Cu	4.233	2.556	2.556	-2.202
7	4	Cu	4.398	1.278	1.278	-4.010
8	4	O	5.112	5.112	0.000	0.000
9	4	Cu	5.437	3.834	3.834	-0.395
10	4	Cu	5.566	5.112	0.000	-2.202
11	8	Cu	5.693	3.834	1.278	-4.010
12	1	Cu	5.817	0.000	0.000	-5.817
13	8	Cu	6.125	5.112	2.556	-2.202
14	4	Cu	6.354	2.556	0.000	-5.817
15	8	Cu	6.529	6.390	1.278	-0.395
16	4	Cu	6.744	3.834	3.834	-4.010
17	4	Cu	6.849	2.556	2.556	-5.817
18	4	O	7.230	5.112	5.112	0.000
19	8	Cu	7.463	6.390	3.834	-0.395

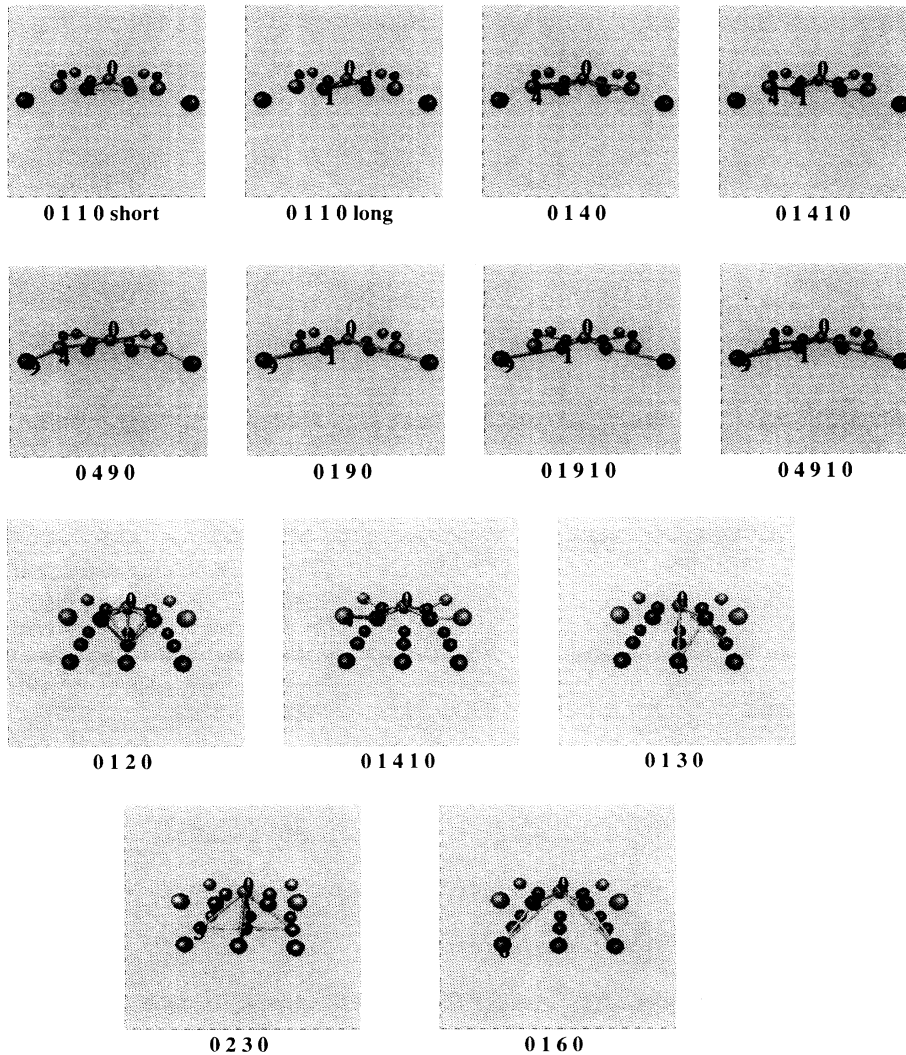


FIG. 3. Schematic diagram of the most important MS paths for Cu(100)c(2 $\times$ 2)O with adsorption in the fourfold hollow site and (a)  $\epsilon \parallel x$  or  $\epsilon \parallel y$  (normal incidence) and (b)  $\epsilon \parallel z$  (grazing incidence). The {0-1-0-1-0} paths cannot readily be depicted and are therefore omitted from (a).

the three inequivalent types of {0-1-0-1-0} path also adding significant weight. This is one of the few geometries investigated in which MS paths involving scattering off the central atom need to be considered. The importance of {0-1-1-0} (long path) MS has previously been reported<sup>10,51</sup> for  $c(2 \times 2)\text{O}/\text{Ni}(100)$ . It is predictable that {0-1-4-0} and {0-1-4-1-0}, with large bond angles ( $155.4^\circ$ ) and therefore small scattering angles ( $24.6^\circ$ ) should give significant contributions. The {0-1-1-0} (short path) contributes mainly because of its short overall path length, which always favors multiple scattering. This path is, however, substantial only at low energies. Paths with large angles generally show less attenuation at high energy. The {0-1-1-0} (long path) contribution has large scattering angles of  $167.7^\circ$  (close to backscattering), associated with relatively strong backscatterers (Cu). This partly offsets the tendency of paths with two backscattering events to be weak. The large scattering angles result in a large bond angle, again  $155.4^\circ$  as for {0-1-4-0}, but the vertex is now at the central atom rather than at the first scattering atom. The maximum angle within a three-atom path is therefore often a good indication of its importance.

In addition to the modification of the second peak, MS gives rise to a strong peak at around  $5.4 \text{ \AA}$ , which is much larger than any SS contributions in the same region. Of the many hundreds of paths which contribute to this peak the most significant are double and triple scattering paths involving shells 1, 4, and 9 (Table III), all of which include bond angles of  $167.7^\circ$ . The high symme-

try of the site ensures that many contributions have the same path length. Some of the most important paths are depicted in Fig. 3(a).

#### $\epsilon||z$ (grazing incidence)

Multiple scattering makes relatively little contribution to the EXAFS spectrum, but is most noticeable in the edge region and between  $k=4.5$  and  $7 \text{ \AA}^{-1}$ . Single-scattering peaks at around  $3.3$  and  $4.3 \text{ \AA}$  are quite strong compared to the first peak, which is due to shells at  $1.85$  and  $2.20 \text{ \AA}$  (four Cu atoms in the top layer and one under the O). Multiple scattering causes some modification of the  $4.3\text{-\AA}$  peak, largely due to the {0-1-6-0} contributions, with its large ( $147.3^\circ$ ) bond angle. As before, the short but nearly equilateral {0-1-2-0} paths are important only near the edge, whereas the paths with large angles such as {0-2-12-0} show less restriction to the edge region. Some of the most important paths for this geometry are depicted in Fig. 3(b) and tabulated in Table IV.

#### B. (110) surface: long bridge site ( $C_{2v}$ symmetry)

##### $\epsilon||x$ (normal incidence, $\epsilon$ perpendicular to bridge bond)

This spectrum is dominated by the first shell. Although MS is relatively large in comparison to SS contributions from the second and higher shells, its overall effect is small (see Table V).

TABLE II. Atomic coordinates for principal shells: O/Cu(110) long bridge site ( $C_{2v}$ ).

Shell	$N$	Atom	$R$ ( $\text{\AA}$ )	$x$ ( $\text{\AA}$ )	$y$ ( $\text{\AA}$ )	$z$ ( $\text{\AA}$ )
1	2	Cu	1.850	1.807	0.000	-0.395
2	2	Cu	2.105	0.000	1.278	-1.673
3	4	Cu	3.155	1.807	2.556	-0.395
4	2	Cu	3.460	1.807	0.000	-2.951
5	4	Cu	4.183	3.615	1.278	-1.673
6	2	Cu	4.183	0.000	3.834	-1.673
7	4	Cu	4.302	1.807	2.556	-2.951
8	2	Cu	4.418	0.000	1.278	-4.229
9	4	O	4.427	3.615	2.556	0.000
10	2	O	5.112	0.000	5.112	0.000
11	2	Cu	5.437	5.422	0.000	-0.395
12	4	Cu	5.437	1.807	5.112	-0.395
13	4	Cu	5.529	3.615	3.834	-1.673
14	4	Cu	5.708	3.615	1.278	-4.229
15	2	Cu	5.708	0.000	3.834	-4.229
16	2	Cu	5.796	1.807	0.000	-5.507
17	4	Cu	6.007	5.422	2.556	-0.395
18	2	Cu	6.173	5.422	0.000	-2.951
19	4	Cu	6.173	1.807	5.112	-2.951
20	4	Cu	6.334	1.807	2.556	-5.507
21	2	Cu	6.605	0.000	6.390	-1.673
22	4	Cu	6.681	5.422	2.556	-2.951
23	4	Cu	6.756	3.615	3.834	-4.229
24	2	Cu	6.904	0.000	1.278	-6.785
25	2	O	7.230	7.230	0.000	0.000
26	4	Cu	7.463	5.422	5.112	-0.395

$\epsilon||y$  (normal incidence,  $\epsilon$  parallel to bridge bond)

Multiple scattering quite strongly affects the EXAFS spectrum near the edge and around  $k = 5 \text{ \AA}^{-1}$ . Inclusion of MS would be essential in any attempt to fit structure beyond the first two peaks. A large number of paths, each making a small individual contribution, is required to model the full MS calculation accurately—more than for any other geometry we have considered. Most of the features can however be accounted for by including only the dominant paths which are {0-1-3-0}, {0-2-3-0}, {0-2-6-0}, {0-2-7-0}, and {0-3-13-0}.

 $\epsilon||z$  (grazing incidence)

Multiple scattering makes some difference to the EXAFS spectrum around  $k = 5 \text{ \AA}^{-1}$ , although the effect on the Fourier transform is not large.

## C. Calculation with a limited number of paths

In general, spectra can be reproduced to a high degree of accuracy by including only a few groups of paths out of the thousands included in the initial calculation. Such paths are listed in Tables III–VII, with an indication of the importance of each path crudely given by the maximum of  $\chi(k)k^2$  at any value of  $k$  in the range  $1-13 \text{ \AA}^{-1}$ . In Fig. 4 is shown a comparison of a limited calculation with one including all terms, for the hypothetical  $c(2 \times 2)$

TABLE III. The significant MS and SS paths for O/Cu(100) hollow site ( $C_{4v}$ ) with  $\epsilon||x$  or  $\epsilon||y$  (normal incidence).  $N$  denotes the number of equivalent paths, and the intensity is the maximum of  $\chi(k)k^2$  at any value of  $k$  in the range  $1-13 \text{ \AA}^{-1}$ . The path is labeled by its index introduced above (Ref. 34). The length is the total photoelectron path length, and the angle is the largest bond angle involved in the path, where this is a useful guide to its likely importance, i.e., when up to three types of scattering atom are involved. An asterisk (\*) in the angle column indicates the SS terms.

$N$	Intensity	Path	Length ( $\text{\AA}$ )	Angle ( $^\circ$ )
4	1.2060	0-1-0	3.700	*
8	0.0975	0-1-1-0	6.256	87.4
4	0.1218	0-3-0	6.748	*
4	0.1181	0-4-0	7.230	*
4	0.1285	0-1-1-0	7.315	155.4
8	0.2238	0-1-4-0	7.315	155.4
4	0.1593	0-1-0-1-0	7.400	0.0
4	0.1635	0-1-0-1-0	7.400	155.4
8	0.0969	0-1-0-1-0	7.400	87.4
4	0.1520	0-1-4-1-0	7.400	155.4
8	0.2884	0-5-0	8.121	*
4	0.0945	0-6-0	8.465	*
16	0.1417	0-1-5-0	8.467	133.7
8	0.0885	0-1-6-0	8.639	147.3
8	0.1306	0-4-9-0	10.901	167.7
8	0.1752	0-1-9-0	10.901	167.7
4	0.0957	0-1-9-1-0	10.930	167.7
8	0.4782	0-4-9-1-0	10.930	
8	0.1294	0-1-4-9-1-0	11.015	

TABLE IV. Significant scattering paths for O/Cu(100) hollow site ( $C_{4v}$ ) with  $\epsilon||z$  (grazing incidence).

$N$	Intensity	Path	Length ( $\text{\AA}$ )	Angle ( $^\circ$ )
1	0.4558	0-2-0	4.404	*
8	0.1447	0-1-2-0	6.608	77.7
4	0.1828	0-3-0	6.748	*
4	0.0657	0-1-4-1-0	7.400	155.4
16	0.0904	0-1-3-0	7.780	98.7
8	0.0597	0-2-3-0	8.132	90.0
4	0.0698	0-6-0	8.465	*
8	0.0600	0-1-6-0	8.639	147.3
4	0.1991	0-7-0	8.796	*
8	0.0996	0-2-7-0	9.156	135.0
16	0.0505	0-1-3-0	9.651	112.6
16	0.0360	0-3-7-0	10.328	94.7
16	0.0518	0-3-11-0	11.623	147.2
2	0.0802	0-2-12-0	11.634	180.0

coverage of O on Cu(100) with (a)  $\epsilon||x$  or  $\epsilon||y$  (normal incidence) and (b)  $\epsilon||z$  (grazing incidence). The limited calculation included 124 paths for  $\epsilon||x$  and 115 paths for  $\epsilon||z$ . These paths were selected after performing the full calculation, tabulating the contribution of each path and summing the spectra of those that made a significant effect. Some of the multiple-scattering components used in Fig. 4(a) together with representative single-scattering terms are shown in Fig. 5. The reduced list of paths allows an excellent approximation to the high-energy region but for both polarization directions some discrepancies remain in the near-edge region. These are largest for  $\epsilon||x$  (normal incidence), which showed the largest difference between the exact and the approximate spectra of all the cases we studied. However, the influence on a structural determination of the lack of agreement in the edge region is small, as seen from the Fourier transforms in Fig. 4 which show far greater consistency than those for single scattering in Fig. 2. In particular the large

TABLE V. Significant scattering paths for O/Cu(110) long bridge site ( $C_{2v}$ ) with  $\epsilon||x$  (normal incidence,  $\epsilon$  perpendicular to bridge bond).

$N$	Intensity	Path	Length ( $\text{\AA}$ )	Angle ( $^\circ$ )
2	1.2394	0-1-0	3.700	*
2	0.0626	0-2-0	4.210	*
4	0.1683	0-3-0	6.311	*
8	0.0600	0-1-2-0	6.511	80.2
2	0.0557	0-4-0	6.920	*
2	0.1262	0-1-1-0	7.315	155.4
8	0.0707	0-1-3-0	7.561	90.0
4	0.2014	0-5-0	8.366	*
8	0.1727	0-1-5-0	8.589	142.9
4	0.0851	0-9-0	8.854	*
8	0.0448	0-1-3-0	9.432	122.2
4	0.1752	0-1-11-0	10.901	167.7
8	0.0447	0-1-5-0	11.749	139.4
8	0.0404	0-1-17-0	12.285	142.9
4	0.0629	0-1-18-0	12.450	157.1

TABLE VI. Significant scattering paths for O/Cu(110) long bridge site ( $C_{2v}$ ) with  $\epsilon||y$  (normal incidence,  $\epsilon$  parallel to bridge bond).

$N$	Intensity	Path	Length ( $\text{\AA}$ )	Angle ( $^\circ$ )
2	0.1087	0-1-0	3.700	*
2	0.3663	0-2-0	4.210	*
4	0.3422	0-3-0	6.311	*
8	0.0247	0-1-2-0	6.511	80.2
2	0.0170	0-2-2-0	6.766	74.8
8	0.0592	0-1-3-0	7.561	90.0
8	0.0494	0-2-3-0	7.816	84.6
4	0.0240	0-5-0	8.366	*
2	0.1134	0-6-0	8.366	*
2	0.0270	0-2-0-2-0	8.420	0.0
4	0.0861	0-7-0	8.604	*
4	0.0493	0-2-6-0	8.844	127.4
8	0.0495	0-2-7-0	8.963	134.5
2	0.0219	0-2-8-2-0	9.322	142.6
8	0.0267	0-1-9-0	9.432	122.2
8	0.0215	0-3-9-0	9.432	122.2
8	0.0413	0-1-3-0	9.432	122.2
8	0.0276	0-2-3-0	9.688	113.1
8	0.0285	0-3-6-0	9.894	93.6
8	0.0179	0-3-7-0	10.013	97.2
4	0.0197	0-1-6-0	10.460	85.1
8	0.0458	0-3-13-0	11.240	150.8
4	0.0173	0-3-13-3-0	11.423	150.8
8	0.0157	0-3-10-0	11.423	108.2
4	0.0161	0-3-1-3-0	11.423	90.0

peak at around 5.4  $\text{\AA}$ , corresponding to path lengths of around 10.9  $\text{\AA}$ , is completely absent from the SS calculation but is reproduced well by that with the reduced set of MS paths. This peak is largely due to MS contributions involving shell 9, and it can be seen from Fig. 5 that some of the MS terms involving that shell are much

TABLE VII. Significant scattering paths for O/Cu(110) long bridge site ( $C_{2v}$ ) with  $\epsilon||z$  (grazing incidence).

$N$	Intensity	Path	Length ( $\text{\AA}$ )	Angle ( $^\circ$ )
2	0.0957	0-1-0	3.700	*
2	0.6415	0-2-0	4.210	*
8	0.0907	0-1-2-0	6.511	80.2
2	0.0425	0-2-2-0	6.766	74.8
2	0.1511	0-4-0	6.920	*
4	0.0365	0-1-4-0	7.866	102.3
8	0.0629	0-2-4-0	8.121	95.4
4	0.0420	0-5-0	8.366	*
2	0.0210	0-6-0	8.366	*
2	0.0464	0-2-0-2-0	8.420	180.0
8	0.0303	0-1-5-0	8.589	142.9
4	0.1151	0-7-0	8.604	*
2	0.1065	0-8-0	8.835	*
8	0.0690	0-2-7-0	8.963	134.5
4	0.0697	0-2-8-0	9.079	142.6
4	0.0956	0-2-15-0	11.428	172.4
2	0.0721	0-2-15-2-0	11.440	172.4
8	0.0257	0-4-14-0	11.724	142.7
4	0.0241	0-4-16-0	11.812	148.5
8	0.0434	0-2-20-0	12.867	149.7

stronger than the single shell {0-9-0} path. Similarly, several MS paths involving shell 4, the nearest oxygen atoms, are more significant than the SS {0-4-0}. However, Fig. 5 shows that the MS terms are all far weaker than the nearest-neighbor {0-1-0} SS contribution.

In order to make a calculation including MS routinely feasible, it will be necessary to use a means of overcoming the proliferation of paths. To select important paths it is often sufficient to perform a calculation with a low value of  $l_{\max}$  or with the small atom approximation, or by including a filter so that only those likely to be important are calculated in full.<sup>32,52</sup>

#### IV. DISCUSSION

The results show that, in general, spectra are dominated by SS contributions from bonding distances (the first one or two shells). Obvious exceptions are for the Cu(100) bridge and Cu(100) atop sites for  $\epsilon||x$ , where nearest-neighbor bonds are normal to the  $\epsilon$  vector and these shells, which would not contribute to a calculation with an approximate form for the polarization dependence, are significant only near the edge. In the Cu(110) long bridge site with  $\epsilon||y$ , the intensity of the first non-bonding shell is a substantial proportion of that for the dominant shell.

Multiple scattering is relatively weak in most cases, but may be a large proportion of the contribution from non-nearest-neighbor shells. Multiple scattering is dominated by second-, and in some cases, third-order terms. Very few fifth-order terms fall within our path length limit, and none is significant. Some of the fourth-order terms are quite large in the edge region, but they tend to cancel each other out, and terms above third order can safely be ignored when fitting  $k^2$ -weighted spectra, where higher-energy parts of the spectra are emphasized at the expense of the near-edge region. In such spectra, the XANES as well as the EXAFS can be used in all cases if a small number of MS paths is included. Indeed, the ratio of multiple to single scattering is larger at  $k = 5 \text{\AA}^{-1}$  than at the edge for some of the spectra. Where MS is weak the errors introduced by fitting the edge region using SS only are likely to be much smaller than the effect of experimental noise in fitting higher-energy data. It is therefore recommended that the edge region is used in analysis when the background subtraction permits it. It is however important to use the exact curved wave polarization dependence when fitting the edge region, and not an angle-dependent amplitude factor as obtained with the small atom theory.

Failure to include at least the dominant double scattering terms will result in errors in the second shell parameters, which are often used to provide geometric information on an adsorbate site. At least some third-order terms are usually required when large bond angles are involved. Additional paths are necessary if the low- $k$  region is exploited. The fourth- and higher-orders make a relatively small contribution to the near-edge region compared to most bulk metals, allowing both the EXAFS and XANES to be fitted using a reasonable number of terms. For systems with higher disorder than we have assumed here, the effect of longer-range contributions, and the rel-

ative contribution of MS, will be less important.

The energy dependence of paths depends very much on their geometry. Three-atom paths that are approximately equilateral are important only when path lengths are short, and tend to influence only the near-edge region. Paths that include a small scattering angle, or two large ones, show much less energy dependence. Paths of intermediate geometry are much harder to predict. The energy dependence is also clearly related to the order of scattering. The higher the order, the greater the energy dependence, with most fifth-order terms almost entirely confined to the edge region.

From our results we derive guidelines for recognizing important multiple-scattering paths in surface studies.

#### A. Bond distance and polarization dependence

The magnitude of a MS path, relative to a SS path of similar length, is related to the product of the Hankel functions ( $h_l$ ) involved in the propagators. In the asymptotic limit when

$$h_l \sim \frac{1}{kr} \exp(ikr)$$

the relative magnitude of the double and single scattering terms is given by

$$\frac{D}{S} = \frac{2[(1/kR_{0 \rightarrow 1})(1/kR_{1 \rightarrow 2})(1/kR_{2 \rightarrow 0})]}{[(1/kR_{0 \rightarrow 2})(1/kR_{2 \rightarrow 0})]}$$

At  $k = 5 \text{ \AA}^{-1}$  a typical value of  $D/S$  for the fourth shell in an fcc metal is 0.32. For a transition-metal carbonyl  $D/S$  is about 0.60, and moreover, for the very short C-O bond ( $\sim 1.05 \text{ \AA}$ ) the asymptotic approximation is particularly poor, and spherical wave effects will increase even more the ratio of double to single scattering. For comparison, the {0-1-1-0} paths of O/Cu(100) in the hollow site considered here, with  $\epsilon \parallel x$ , give a value for  $D/S$  of 0.16. Of course these values increase at lower  $k$ . The dominant MS paths therefore involve the shortest bonds in the material, here the  $1.85\text{-\AA}$  adsorbate-metal distances.

Our calculations show that the effect of MS is usually weak for  $\epsilon \parallel z$  (grazing incidence), and the polarization dependence tends to select those contributions where the  $\epsilon$  vector is more or less parallel to one of the short bonds. Comparison of Figs. 4(a) and 4(b), or Tables III and IV, illustrates the substantial polarization dependence of MS,

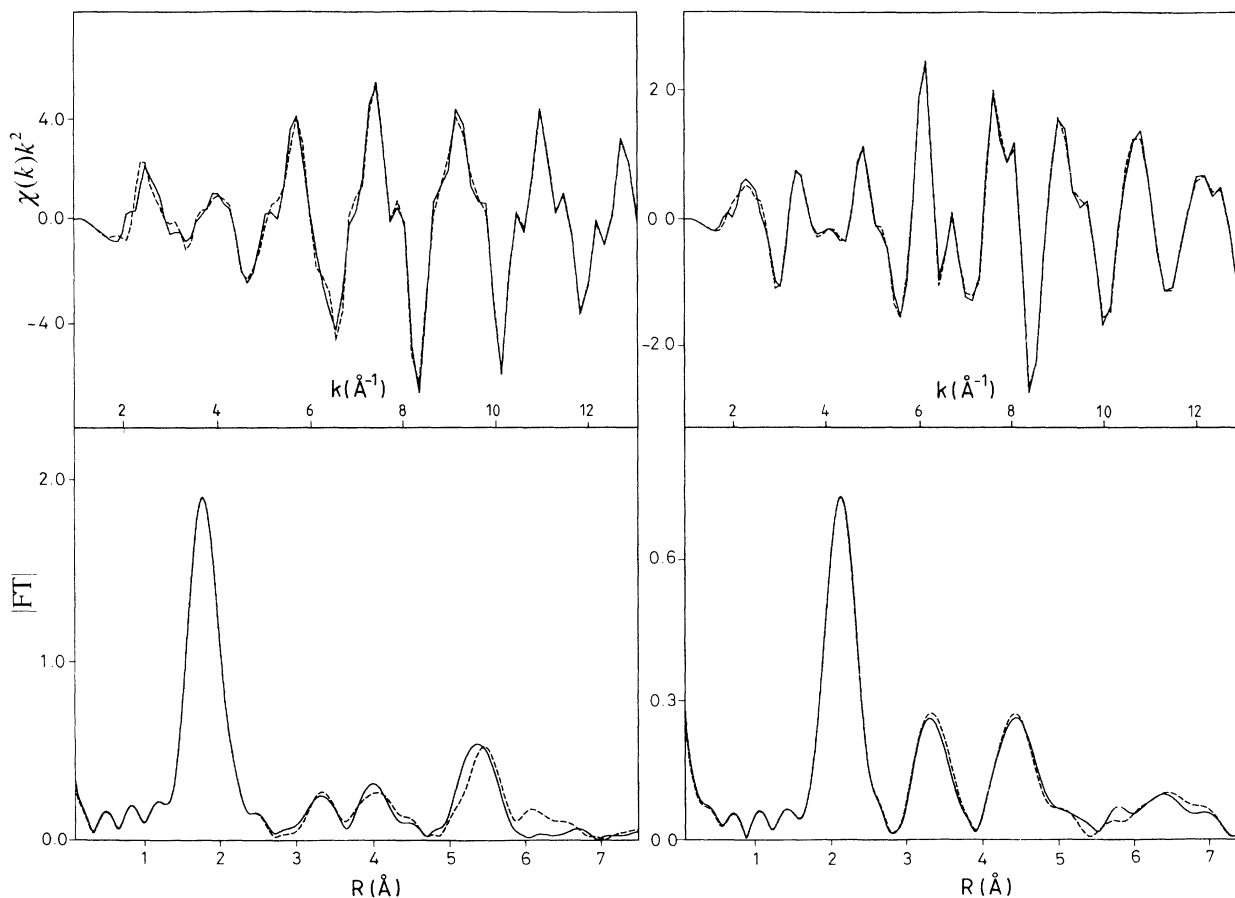


FIG. 4. Calculated EXAFS spectra  $\chi(k)k^2$  and their Fourier transforms, for the hypothetical  $c(2 \times 2)$  coverage of O on Cu(100) with adsorption in the fourfold hollow site and (a)  $\epsilon \parallel x$  or  $\epsilon \parallel y$  (normal incidence) and (b)  $\epsilon \parallel z$  (grazing incidence). A full calculation including all possible paths up to fifth order of multiple scattering is shown by the full line, while the dashed line shows the effect of including only the restricted paths listed in (a) Table III and (b) Table IV.

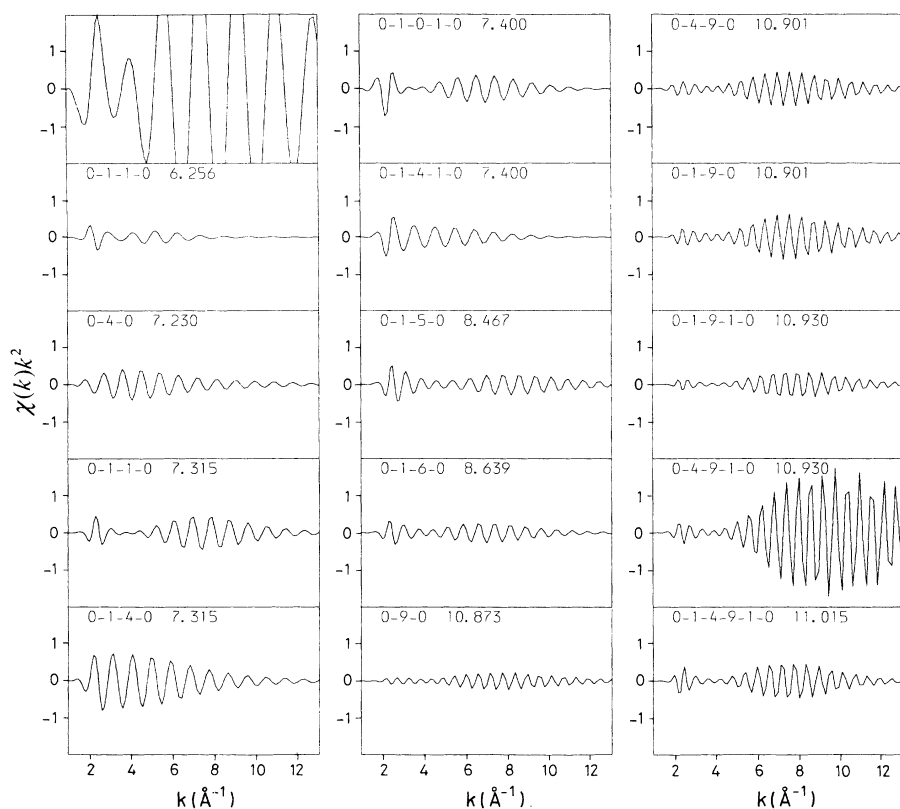


FIG. 5. Calculated EXAFS spectra  $\chi(k)k^2$  for the hypothetical  $c(2 \times 2)$  coverage of O on Cu(100) with adsorption in the fourfold hollow site and  $\epsilon||x$  or  $\epsilon||y$  (normal incidence), as for Fig. 4(a), with the individual scattering paths plotted separately. Each curve is labeled with its index, such as {0-1-4-9-1-0}, indicating the atoms involved in the photoelectron scattering path, and with the path length ( $\text{\AA}$ ). The top left-hand panel is the single scattering {0-1-0} contribution with a path length of 3.70  $\text{\AA}$ . The multiple-scattering calculations are the sum over all equivalent paths. The ordinate axis is the same for all panels, to enable the relative importance of different paths to be assessed.

with the large-angled {0-1-4-1-0} and {0-1-6-0} paths being the only ones that are significant at both normal and grazing incidence. This  $\epsilon$ -vector dependence is likely to be important when analyzing angle-dependent surface EXAFS spectra.

Where MS is significant it may either increase or diminish the intensity of the SS contributions. All the paths in a group of atoms must be considered to determine whether interference will occur between them. For a simple example, consider three collinear atoms 0-*A*-*B*, with both scattering atoms on the same side of the absorber. For the second-neighbor shell the SS (0-*B*-0), double-scattering (0-*A*-*B*-0 and 0-*B*-*A*-0), and dominant triple-scattering (0-*A*-*B*-*A*-0) terms all have the same path length, but differ in phase. Destructive interference will therefore result. However, for the same collinear group with the scattering atoms on opposite sides of the absorber (*A*-0-*B*), this is not the case, and although these paths would normally be weaker, with backscattering events at both *A* and *B*, the lack of interference means their contribution is enhanced. It is of course essential to take these factors into account: Calculating second- or fourth-order terms without third- or fifth-order terms of similar path length for a (0-*A*-*B*) situation results in serious errors.

#### B. Angle and atomic number dependence

The scattering amplitude as a function of angle is given in the asymptotic limit by<sup>4</sup>

$$f(\vartheta) = \frac{1}{ik} \sum_{l=0}^{l_{\max}} (2l+1) P_l(\cos\vartheta) T_l(k),$$

where  $P_l$  is the  $l$ th associated Legendre polynomial. The function  $f(\vartheta)$  peaks in the forward and backscattering directions, and has some minima and maxima at intermediate angles, the details depending on the atom and the electron energy. The details of  $f(\vartheta)$  determine which MS paths are likely to contribute most. When one partial wave dominates the scattering, which tends to happen particularly for light (low-*Z*) atoms and for other atoms at low energies, the angular dependence of  $f(\vartheta)$  is dominated by the angular dependence of  $P_l$ . The isotropic *s*-wave ( $l=0$ ) is always present, but weak, and tends to shift the maxima and minima slightly away from those of  $P_l$ , and also to reduce the magnitude of backscattering relative to forward scattering. For example, oxygen is dominated by  $P_1$  and scatters strongly at forward and backward angles, but nowhere in between. At low energies, copper is dominated by  $P_2$  and thus backscatters strongly, with another maximum close to 90° and minima close to 60° and 120°. At higher energies ( $\geq 25$  eV), the maxima for scattering off copper shift towards 60° and 120°, making the near-equilateral triangular MS paths important. Some typical plots of  $f(\vartheta)$  have been published elsewhere for Cu,<sup>4</sup> Ni,<sup>25</sup> Pt,<sup>53</sup> for Ni and O (Ref. 54), and for a wide range of atoms.<sup>55,56</sup>

Our calculations show that near-equilateral triangle paths tend to be important mainly near to the edge, whereas paths with larger angles give MS contributions extending through the EXAFS region. It is generally true that most of the important paths for MS involve either one small ( $< 45^\circ$ ) or large ( $> 150^\circ$ ) scattering angle. The most favorable geometry for multiple scattering is when forward scattering occurs at a light atom and back-

scattering at a heavy atom. MS effects are likely to be strongest when adsorbate atoms occupy sites close to coplanar with the surface. This, combined with the preferential selection of short bond lengths for MS, tends to mean that MS will be more significant with light adsorbates, their small atomic radii giving short adsorbate-substrate distances and also allowing them to occupy nearly coplanar sites.

### C. Implications for structural studies using surface EXAFS

The importance of MS should be borne in mind for any surface EXAFS investigation where analysis of peaks beyond the first shell is attempted, although longer-range contributions would be less prominent in experimental spectra due to the presence of noise. Variation of experimental parameters such as the polarization angle or the temperature will change the MS contributions, and a phenomenological comparison of the intensities of peaks in Fourier transformed spectra is fraught with danger. However, with care, a proper consideration of the MS effects can maximize the information content of the technique. For instance, contributions up to the fifth shell have been analyzed for S or Cl adsorbed in the fourfold hollow site on Cu or Ni(100) surfaces,<sup>57</sup> the authors stating that "possible MS effects were carefully investigated and found to be negligible." Our calculations show a large intensity of MS at high  $k$  for O in the similarly symmetrical Cu(100) fourfold hollow site with x rays at normal incidence. Both of the factors  $A$  and  $B$  mentioned above will tend to make the S and Cl adsorbate systems less susceptible to MS: The bond length is greater [2.23 Å for S on Ni(100)], making the adsorbate sit higher above the surface plane, thus increasing the scattering angles. The analysis of bulk Pt,<sup>53</sup> with a nearest-neighbor distance of 2.77 Å, also shows the influence of the increased path length in diminishing the MS effects.

An important factor in the strength of MS is the symmetry of the site. Departure from symmetry will result in interference between MS terms rather than the reinforcement seen in our model geometries. The presence of MS peaks at high- $R$  in an experimental spectrum is therefore a useful indication of high symmetry and relatively long-range order in surface structures. Some adsorbates have been suggested to occupy asymmetric sites, such as that off center from the hollow site for  $c(2 \times 2)\text{O}/\text{Ni}(100)$  (Ref. 58) and disordered  $\text{O}/\text{Ni}(100)$  (Ref. 59), and a multiple scattering analysis of high-quality surface EXAFS data might shed light on this and similar problems. In

addition, several of the significant MS paths in our calculations involve scattering off other oxygen atoms, and these contributions will obviously diminish if the adsorbate coverage is reduced below the half-monolayer that we assumed.

## V. CONCLUSIONS

Multiple scattering can be important for light element adsorbates for certain polarization directions in hollow, long bridge, and atop sites on transition-metal surfaces. The condition for maximizing the contribution is that the  $\epsilon$  vector is roughly parallel to the nearest-neighbor distance. Thus, there can be a strong polarization dependence to the MS effects. Multiple scattering will diminish if site symmetry is lost. Second-, and sometimes third-order contributions are more important than higher orders, and when fitting  $k^2$ -weighted spectra, the multiple-scattering contribution in the  $k=3-6\text{\AA}^{-1}$  region matters as much as nearer to the edge, at least in the case of Cu where there is a weak minimum in the scattering amplitude. Specific features due to multiple scattering are most likely to be seen in this spectral region, where the single-scattering amplitude may be reduced by interference between first and higher shells. It is important to include multiple-scattering effects in curve fitting for these situations, and by doing so it becomes feasible to fit the data from the absorption edge upwards, provided that theoretical phase shifts are adequate.

The improvement in fit resulting from the implementation of multiple scattering is certainly not sufficient to introduce additional variables in the analysis. Indeed, if all the shell radii required to model the remote shells were introduced, the refinement of variables would certainly be overdetermined. In order to circumvent this we recommend that for each structural model considered for EXAFS of adsorbates on single-crystal substrates, a constrained refinement scheme is used. Only a few parameters should be allowed to vary, such as the adsorbate-substrate distance, the surface relaxation, and the displacement of the adsorbate from a high-symmetry site. In this way, multiple scattering will ensure a more rigorous test of the model, as no refinement of angle parameters will be required. We have recently implemented such a scheme.<sup>60</sup>

## ACKNOWLEDGMENT

We are pleased to thank S. J. Gurman for useful discussions.

<sup>1</sup>D. Norman, *J. Phys. C* **19**, 3273 (1986).

<sup>2</sup>J. Stöhr, in *Principles, Applications, Techniques of EXAFS, SEXAFS, and XANES*, edited by D. C. Koningsberger and R. Prins (Wiley, New York, 1988).

<sup>3</sup>P. H. Citrin, *J. Phys. (Paris) Colloq.* **47**, C 8-437 (1986).

<sup>4</sup>P. A. Lee and J. B. Pendry, *Phys. Rev. B* **11**, 2795 (1975).

<sup>5</sup>P. J. Durham, J. B. Pendry, and C. H. Hodges, *Comput. Phys. Commun.* **25**, 193 (1982).

<sup>6</sup>D. Norman, J. Stöhr, R. Jaeger, P. J. Durham, and J. B. Pen-

dry, *Phys. Rev. Lett.* **51**, 2052 (1983).

<sup>7</sup>D. R. Warburton, G. Thornton, D. Norman, C. H. Richardson, and R. McGrath, *Phys. Rev. B* **43**, 12 289 (1991).

<sup>8</sup>S. J. Gurman, N. Binsted, and I. Ross, *J. Phys. C* **19**, 1845 (1986).

<sup>9</sup>A. Filipponi, A. Di Cicco, R. Zanoni, M. Bellatreccia, V. Sessa, C. Dossi, and R. Psaro, *Chem. Phys. Lett.* **184**, 485 (1991).

<sup>10</sup>D. Arvanitis, K. Baberschke, and L. Wenzel, *Phys. Rev. B* **37**, 7143 (1988).

- <sup>11</sup>J. J. Boland, S. E. Crane, and J. Baldeschweiler, *J. Chem. Phys.* **77**, 142 (1982).
- <sup>12</sup>J. Stöhr and K. R. Bauchspiess, *Phys. Rev. Lett.* **67**, 3376 (1991).
- <sup>13</sup>N. Binsted and D. Norman, *Jpn. J. Appl. Phys., Suppl.* **32-2**, 342 (1993).
- <sup>14</sup>S. J. Gurman, *J. Phys. C* **21**, 3699 (1988).
- <sup>15</sup>J. J. Rehr, J. Mustre de Leon, S. I. Zabinsky, and R. C. Albers, *J. Amer. Chem. Soc.* **113**, 5135 (1991).
- <sup>16</sup>W. L. Schaich, *Phys. Rev. B* **29**, 6513 (1984).
- <sup>17</sup>J. J. Barton and D. A. Shirley, *Phys. Rev. B* **32**, 1906 (1985).
- <sup>18</sup>J. J. Rehr and R. C. Albers, *Phys. Rev. B* **41**, 8139 (1990).
- <sup>19</sup>J. J. Barton and D. A. Shirley, *Phys. Rev. A* **32**, 1019 (1985).
- <sup>20</sup>V. Fritzsche and P. Rennert, *Phys. Status Solidi B* **135**, 49 (1986).
- <sup>21</sup>V. Fritzsche, *J. Phys. Condens. Matter* **2**, 1413 (1990).
- <sup>22</sup>V. Fritzsche, *J. Electron Spectrosc. Rel. Phenom.* **58**, 299 (1992).
- <sup>23</sup>J. E. Muller and W. L. Schaich, *Phys. Rev. B* **27**, 6489 (1983).
- <sup>24</sup>It is unfortunate that copper metal is frequently chosen as the test case for calculations of electron scattering. In the low- $k$  region, it is close to free-electron-like and its scattering is so weak that SS often appears sufficient to give a good fit.
- <sup>25</sup>J. J. Barton and D. A. Shirley, *Phys. Rev. B* **32**, 1892 (1985).
- <sup>26</sup>P. Rennert and Nguyen Van Hung, *Phys. Status Solidi B* **148**, 49 (1988).
- <sup>27</sup>C. Brouder, M. F. Ruiz Lopez, R. F. Pettifer, M. Benfatto, and C. R. Natoli, *Phys. Rev. B* **39**, 1488 (1989).
- <sup>28</sup>M. Benfatto, C. R. Natoli, C. Brouder, R. F. Pettifer, and M. F. Ruiz Lopez, *Phys. Rev. B* **39**, 1939 (1989).
- <sup>29</sup>D. D. Vvedensky, D. K. Saldin, and J. B. Pendry, *Comput. Phys. Commun.* **40**, 421 (1986).
- <sup>30</sup>N. Binsted, G. N. Greaves, and C. M. B. Henderson, *Prog. Exptl. Petr.* **6**, 66 (1984).
- <sup>31</sup>N. Binsted, S. L. Cook, J. Evans, G. N. Greaves, and R. J. Price, *J. Amer. Chem. Soc.* **109**, 369 (1987).
- <sup>32</sup>J. J. Rehr, R. C. Albers, and S. I. Zabinsky, *Phys. Rev. Lett.* **69**, 3397 (1992).
- <sup>33</sup>N. Binsted (unpublished).
- <sup>34</sup>Here we use "path" to mean one MS contribution, like  $0 \rightarrow 1 \rightarrow 4 \rightarrow 0$ , where the numbers refer to atoms in different shells around the absorbing atom (0), and the arrows indicate the direction of propagation of the photoelectron. Often there are many equivalent such paths, and we introduce a nomenclature akin to that for Miller indices, with  $\{0-i-j-0\}$  meaning all paths of the  $0 \rightarrow i \rightarrow j \rightarrow 0$  type, and  $(0-i-j-0)$  being used for a specific path. Sometimes there may be inequivalent paths involving atoms in the same shells, and it is assumed in this paper that the atoms involved are those that generate the shortest path length unless otherwise specified.
- <sup>35</sup>J. M. Tranquada and R. Ingalls, *Phys. Rev. B* **28**, 3520 (1983).
- <sup>36</sup>I. R. Beattie, W. Levason, N. Binsted, J. S. Ogdan, M. D. Spicer, and N. A. Young, *High Temp. Sci.* **26**, 71 (1990).
- <sup>37</sup>L. Tröger, D. Arvanitis, J. J. Rehr, T. Lederer, T. Yokoyama, K. Baberschke, and E. Zschech, *Jpn. J. Appl. Phys. Suppl.* **32-2**, 137 (1993).
- <sup>38</sup>N. Binsted, R. W. Strange, and S. S. Hasnain, *Biochem.* **31**, 1211 (1992).
- <sup>39</sup>L. F. Mattheis, *Phys. Rev. B* **8**, 3719 (1973).
- <sup>40</sup>G. Beni, P. A. Lee, and P. M. Platzman, *Phys. Rev. B* **13**, 5170 (1976).
- <sup>41</sup>P. A. Lee and G. Beni, *Phys. Rev. B* **15**, 2862 (1977).
- <sup>42</sup>L. Hedin and S. Lundqvist, *Solid State Physics: Advances in Research and Applications*, edited by F. Seitz, D. Turnbull, and H. Ehrenreich (Academic, New York, 1969), Vol. 23, p. 1.
- <sup>43</sup>J. Mustre de Leon, Y. Yacoby, E. A. Stern, and J. J. Rehr, *Phys. Rev. B* **42**, 10843 (1990).
- <sup>44</sup>J. Mustre de Leon, J. J. Rehr, S. I. Zabinsky, and R. C. Albers, *Phys. Rev. B* **44**, 4146 (1991).
- <sup>45</sup>D. R. Warburton, D. Purdie, C. A. Muryn, N. S. Prakash, K. Prabhakaran, G. Thornton, R. A. D. Patrick, and D. Norman, *Phys. Rev. B* **45**, 12043 (1992).
- <sup>46</sup>N. Binsted, D. Norman, and G. Thornton (unpublished).
- <sup>47</sup>L. I. Schiff, *Quantum Mechanics* (McGraw-Hill, New York, 1968).
- <sup>48</sup>S. J. Gurman, N. Binsted, and I. Ross, *J. Phys. C* **17**, 143 (1984).
- <sup>49</sup>For a good summary of the structural possibilities for O/Cu(100), see M. C. Asensio, M. J. Ashwin, A. L. D. Kilcoyne, D. P. Woodruff, A. W. Robinson, Th. Lindner, J. S. Somers, D. E. Ricken, and A. M. Bradshaw, *Surf. Sci.* **236**, 1 (1990); for O/Cu(110), a useful summary is that by S. R. Parkin, H. C. Zeng, M. Y. Zhou, and K. A. R. Mitchell, *Phys. Rev. B* **41**, 5432 (1990).
- <sup>50</sup>O. Keski-Rahkonen and M. O. Krause, *At. Data Nucl. Data Tables* **14**, 140 (1974).
- <sup>51</sup>K. Baberschke, in *The Structure of Surfaces II*, edited by J. F. van der Veen and M. A. Van Hove (Springer-Verlag, Berlin, 1988), p. 174.
- <sup>52</sup>J. J. Rehr, *Jpn. J. Appl. Phys. Suppl.* **32-2**, 8 (1993).
- <sup>53</sup>V. A. Biebesheimer, E. C. Marques, D. R. Sandstrom, F. W. Lytle, and R. B. Gregor, *J. Chem. Phys.* **81**, 2599 (1984).
- <sup>54</sup>M.-L. Xu, J. J. Barton, and M. A. Van Hove, *Phys. Rev. B* **39**, 8275 (1989).
- <sup>55</sup>M. Fink, M. R. Martin, and G. A. Somorjai, *Surf. Sci.* **29**, 303 (1972).
- <sup>56</sup>M. B. Webb and M. G. Lagally, *Solid State Physics: Advances in Research and Applications*, edited by H. Ehrenreich, F. Seitz, and D. Turnbull (Academic, New York, 1973), Vol. 28, p. 301.
- <sup>57</sup>F. Sette, T. Hashizume, F. Comin, A. A. MacDowell, and P. H. Citrin, *Phys. Rev. Lett.* **61**, 1384 (1988).
- <sup>58</sup>J. E. Demuth, N. J. DiNardo, and G. S. Cargill III, *Phys. Rev. Lett.* **50**, 1373 (1983).
- <sup>59</sup>U. Starke, P. L. de Andres, D. K. Saldin, K. Heinz, and J. B. Pendry, *Phys. Rev. B* **38**, 12277 (1988).
- <sup>60</sup>N. Binsted and D. Norman, in *The Structure of Surfaces IV*, edited by X. D. Xie, S. Y. Tong, and M. A. Van Hove (World Scientific, Singapore, in press).

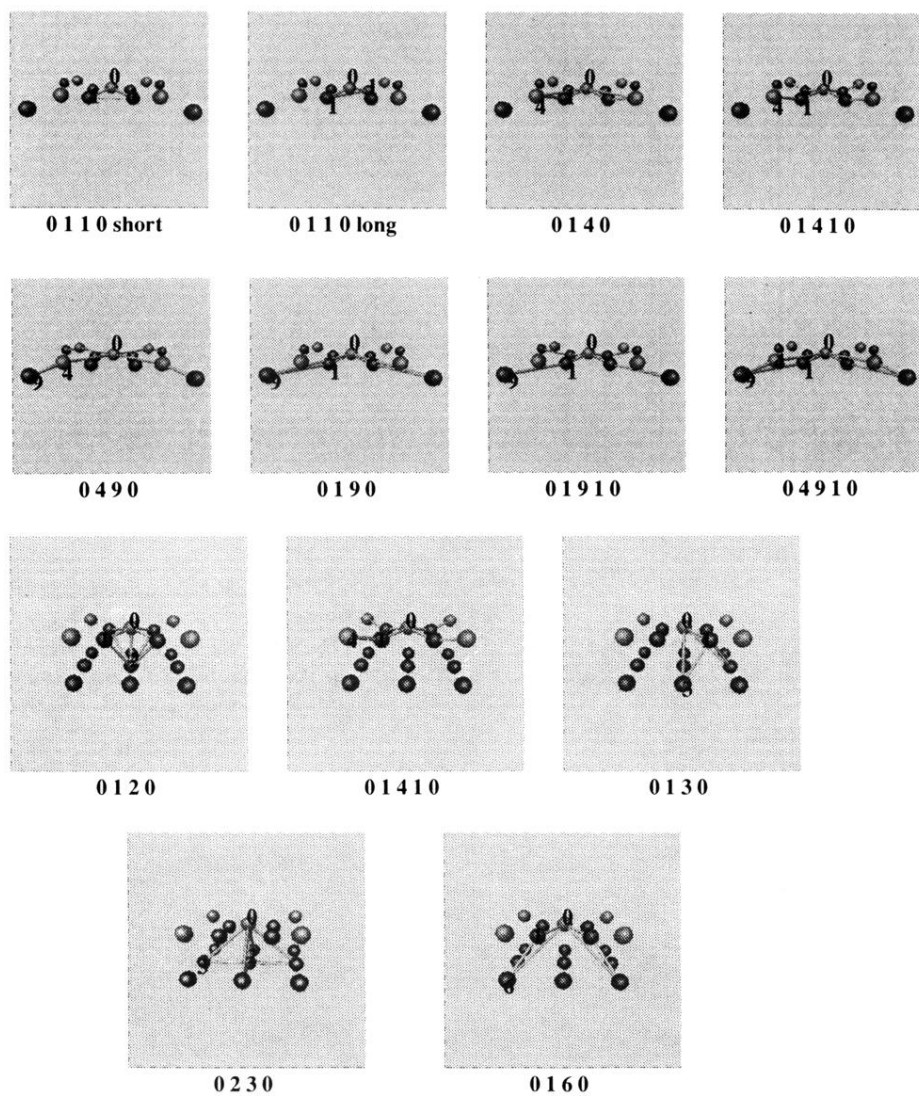


FIG. 3. Schematic diagram of the most important MS paths for  $\text{Cu}(100)c(2 \times 2)\text{O}$  with adsorption in the fourfold hollow site and (a)  $\epsilon \parallel x$  or  $\epsilon \parallel y$  (normal incidence) and (b)  $\epsilon \parallel z$  (grazing incidence). The  $\{0-1-0-1-0\}$  paths cannot readily be depicted and are therefore omitted from (a).